

Inclusive h_c production and energy spectrum from e^+e^- annihilation at Super B factory

Qing-Feng Sun ^{*,1,2} Yu Jia ^{†,2} Xiaohui Liu ^{‡,3} and Ruilin Zhu ^{§4}

¹*Department of Modern Physics, University of Science and Technology of China, Hefei, Anhui 230026, China*

²*Institute of High Energy Physics, Chinese Academy of Sciences, Beijing 100049, China*

³*Center of Advanced Quantum Studies and Department of Physics, Beijing Normal University, Beijing, 100875, China*

⁴*Department of Physics and Institute of Theoretical Physics, Nanjing Normal University, Nanjing, Jiangsu 210023, China*

(Dated: December 3, 2024)

Abstract

We calculate the next-to-leading order (NLO) radiative correction to the color-octet h_c inclusive production in e^+e^- annihilation at Super B factory, within the nonrelativistic QCD (NRQCD) factorization scheme. The analytical expression for the NLO short-distance coefficient accompanying the color-octet production operator $\mathcal{O}_8^{h_c}(^1S_0)$ is obtained after including both virtual and real corrections. The NLO correction from the color-octet channel is found to be positive and substantial. The h_c energy spectrum from our NLO prediction is plagued with the end-point divergence, thus unphysical. With the aid of the soft-collinear effective theory (SCET), those large threshold logarithms are resummed to the next-to-leading logarithmic (NLL) accuracy. Consequently, we obtain the well-behaved predictions for the h_c energy spectrum in the whole kinematic range, which awaits the examination in the forthcoming Belle 2 experiment.

PACS numbers: 12.38.Bx, 12.38.Cy, 14.40.Pq, 12.39.Hg

* qfsun@mail.ustc.edu.cn

† jiay@ihep.ac.cn

‡ xiliu@bnu.edu.cn

§ rlzhu@njnu.edu.cn

I. INTRODUCTION

The $h_c(1P)$ meson, the lowest-lying spin-singlet P -wave charmonium, is the last member found among the charmonium family below open threshold. The first hint about its existence was reported in the process $p\bar{p} \rightarrow h_c(\rightarrow J/\psi\pi^0)$ by the Fermilab E760 experiment in 1992 [1]. Finally in 2005, the h_c state was firmly established through the process $p\bar{p} \rightarrow h_c \rightarrow \eta_c\gamma$ in Fermilab E835 experiment [2], as well as through the isospin-violating charmonium transition $\psi(2S) \rightarrow h_c(\rightarrow \eta_c\gamma) + \pi^0$ in CLEO-c experiment [3]. Later this decay chain was confirmed in the BESIII experiment with much large data sample [4, 5]. To date, the most accurately measured mass and width of h_c are $M_{h_c} = 3525.38 \pm 0.11$ MeV and $\Gamma = 0.7 \pm 0.4$ MeV [6]. Two exclusive decay channels, the dominant $E1$ transition $h_c \rightarrow \eta_c\gamma$, and the OZI-suppressed annihilation decay $h_c \rightarrow 2\pi^+2\pi^-\pi^0$, have been measured, with the corresponding branching fractions $\mathcal{B}(h_c \rightarrow \eta_c\gamma) = (51 \pm 6)\%$, and $\mathcal{B}(h_c \rightarrow 2\pi^+2\pi^-\pi^0) = (2.2^{+0.8}_{-0.7})\%$, respectively [6]. It is worth mentioning that, the 1P_1 counterparts in the bottomonium family, the $h_b(1P, 2P)$ mesons, have also been recently established via di-pion transition from $\Upsilon(5S)$ in the Belle experiment [7].

It is interesting to ask whether one can possibly understand various dynamical aspects of the h_c meson from the first principles of QCD. In fact, nonrelativistic QCD (NRQCD) [8], the modern effective field theory to describe the slowly-moving heavy quark-antiquark system, is the appropriate model-independent framework to tackle a multi-scale system exemplified by the charmonium state h_c . Furthermore, the NRQCD factorization approach [9], originally developed by Bodwin, Braaten and Lepage, provides a powerful and systematic language to describe the inclusive quakonium production and decay processes, which has been fruitfully applied to uncountable charmonium phenomenology in the past two decades [10].

For the dominant decay channel $h_c \rightarrow \eta_c\gamma$, there have been many preceding studies based on the classic multi-pole expansion picture in the quark potential models [11]. Recently, the radiative and relativistic corrections to the inclusive hadronic widths of $h_{c,b}$ have been investigated in the NRQCD factorization framework [12]. On the other hand, h_c production in various collision environments have also been extensively investigated in recent years. For instance, h_c inclusive production in B meson decay [13, 14], h_c photoproduction [15], h_c hadroproduction [16–18], inclusive h_c production from e^+e^- annihilation [19, 20], exclusive h_c production from Z^0 decay [21], via the double charmonium production in e^+e^- annihilation [22] as well as from $\Upsilon(nS)$ decay [23].

The hadroproduction rate of h_c is significant at LHC experiment due to huge partonic luminosity (A recent computation indicates that the gluon-to- h_c fragmentation probability may reach the order 10^{-6} [24]). In sharp contrast to $J/\psi(\psi')$ hadroproduction [25–29], unfortunately it is rather challenging to reconstruct the h_c events via its decay into $\eta_c\gamma$ due to the tremendous background at hadron collision experiments. In contrast, tagging h_c is much more tractable in the e^+e^- machines than in hadron colliders. For example, the exclusive h_c production process $e^+e^- \rightarrow h_c\pi^+\pi^-$ at center-of-mass energy $\sqrt{s} = 4.170$ GeV has been studied by the CLEO Collaboration, with the cross section measured to be $15.6 \pm 2.3 \pm 1.9 \pm 3.0$ pb [30]. They also found evidence for the process $e^+ + e^- \rightarrow h_c + \eta$ at 3σ confidence level. As a byproduct of studying this exclusive h_c production channel, BESIII recently have found two charmonium-like resonances, namely the $Y(4220)$ and $Y(4390)$ [31].

The forthcoming Belle2 experiment will accumulate a tremendous dataset near $\Upsilon(4S)$ energy. In this paper, we will focus on the inclusive h_c production in e^+e^- annihilation at $\sqrt{s} \approx 10.6$ GeV. In the previous work, both the short-distance coefficients were computed for

both color-singlet and color-octet channels at the lowest order (LO) in α_s [19, 20], and it was found the latter makes an overwhelming contribution with respect to the former. Therefore, it is helpful to know the next-to-leading order (NLO) correction in the color-octet channel. Moreover, to expedite the experimental search for h_c , it is crucial to predict not only the total h_c production rate, but also the differential h_c energy spectrum.

The LO color-octet contribution to the h_c spectrum is simply a δ -function. After including the real correction in the color-octet channel, the energy spectrum then becomes continuous over all allowed domain, however turns out to be singular near the upper endpoint, due to the radiation of the soft and collinear gluons. This signals a breakdown of fixed-order QCD prediction and failure of NRQCD expansion near this kinematic endpoint region. The aim of this work is thus two fold. First we extend the LO color-octet short-distance coefficient [19] to the NLO in α_s , in a fully analytical manner. Secondly, we follow the recipe of the resumming large logarithms in the color-octet channel for the process $e^+e^- \rightarrow J/\psi + X$ near the endpoint regime [32], which was formulated in the context of the soft-collinear effective theory (SCET) [33–38], to tame the endpoint singularity encountered in our case and finally predict a well-behaved h_c energy spectrum. We hope our prediction will provide some useful guidance for future establishing h_c in the Belle 2 experiment.

The rest of the paper is distributed as follows. In Sec. II, fixed-order calculation for the SDCs are presented within the NRQCD factorization framework. We first review the existing leading-order results for both color-singlet and octet channels. Then we show how to analytically deduce the NLO corrections to the color-octet contributions, including both virtual and real corrections. In Sec. IV, within the SCET framework, we show how to resum the large threshold logarithms to the next-to-leading logarithmic accuracy. In Sec. V, we present our numerical results for the total h_c production rate and h_c differential energy spectrum. We also discuss the observation prospects of the $h_c(1P, 2P)$ in the forthcoming Belle 2 experiment. Finally we present summarize in Sec. VI. In the Appendix, we expound how we carry out the three-body phase space in $d = 4 - 2\epsilon$ dimensions to isolate the IR divergences.

II. NRQCD FACTORIZATION AND LO SHORT-DISTANCE COEFFICIENTS

A. NRQCD factorization for h_c production

Heavy quarkonium is a bound system predominantly composed of a pair of nonrelativistic heavy quark and antiquark. For charmonium, the typical velocity of the charm quark inside a charmonium is roughly $v^2 \approx 0.3$, so NRQCD expansion may not perform particularly well. According to the NRQCD factorization [9], the inclusive production rate of h_c can be factorized as a sum of products of the perturbatively-calculable short-distance coefficients (SDCs) and the non-perturbative NRQCD long-distance matrix elements (LDMEs), which are organized in power series of v . At the lowest order in v , the differential cross section for producing h_c can be written as [9]

$$d\sigma[e^+e^- \rightarrow h_c + X] = \frac{dF_1(\mu_\Lambda)}{m_c^4} \langle \mathcal{O}_1^{h_c}(^1P_1) \rangle + \frac{dF_8}{m_c^2} \langle \mathcal{O}_8^{h_c}(^1S_0)(\mu_\Lambda) \rangle + \cdots, \quad (1)$$

where the SDCs F_1 and F_8 can be calculated order by order in α_s , $\langle \mathcal{O}_1^{h_c}(^1P_1) \rangle$ and $\langle \mathcal{O}_8^{h_c}(^1S_0) \rangle$ are the color-singlet and color-octet NRQCD production LDMEs. The corresponding h_c

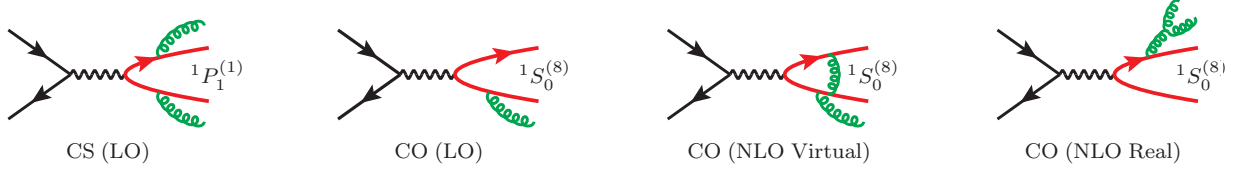


Figure 1: Representative Feynman diagrams for the $c\bar{c}(n)$ production from e^+e^- annihilation, for $n = {}^1S_0^{(8)}$ and ${}^1P_1^{(1)}$.

production operators in NRQCD are defined as [9]¹

$$\mathcal{O}_1^{h_c}({}^1P_1) = \chi^\dagger \left(-\frac{i}{2} \overleftrightarrow{\mathbf{D}} \right) \psi \sum_X |h_c + X\rangle \cdot \langle h_c + X | \psi^\dagger \left(-\frac{i}{2} \overleftrightarrow{\mathbf{D}} \right) \chi, \quad (2a)$$

$$\mathcal{O}_8^{h_c}({}^1S_0) = \chi^\dagger T^a \psi \sum_X |h_c + X\rangle \langle h_c + X | \psi^\dagger T^a \chi, \quad (2b)$$

where ψ and χ denotes the Pauli spinor fields that annihilate a heavy quark and create a heavy antiquark, respectively. $\overleftrightarrow{\mathbf{D}}$ represents the left-right symmetric spatial component of the covariant derivative D_μ , and T^a ($a = 1, \dots, 8$) signifies the generator in the fundamental representation of the $SU(3)_c$ group. The μ_Λ refers to the NRQCD factorization scale, which lies in the range $m_c v \leq \mu_\Lambda \leq m_c$. These two NRQCD production operators are interconnected through the following renormalization group equation [9]:

$$\frac{d}{d \ln \mu_\Lambda^2} \langle \mathcal{O}_8^{h_c}({}^1S_0)(\mu_\Lambda) \rangle = \frac{2\alpha_s C_F}{3\pi N_c m^2} \langle \mathcal{O}_1^{h_c}({}^1P_1) \rangle. \quad (3)$$

Being the infrared-finite SDCs, dF_1 and dF_8 are insensitive to the long-distance hadronization effects, thus can be determined through the standard perturbative matching procedure. One can replace the physical h_c state in (1) by the free on-shell $c\bar{c}$ pairs with quantum numbers ${}^1S_0^{(8)}$ and ${}^1P_1^{(1)}$, computing both sides of (1), demanding both perturbative QCD and perturbative NRQCD to generate identical results. Ultimately, one can solve these two linear equations to ascertain the two SDCs, order by order in α_s . Here we stress that it is crucial to include the color-octet contribution, otherwise the uncanceled IR divergences emerging from the color-singlet channel would impede the predictive power of NRQCD. For the computation in the QCD side, it is convenient to employ the covariant projection technique [41] to project the $c\bar{c}$ amplitude onto the intended ${}^{2S+1}L_J$ state. Throughout this work, Dimensional Regularization (DR), that is, to work in the spacetime dimensions $d = 4 - 2\epsilon$, is adopted to regularize both UV and IR divergences.

A kinematical simplification also arises from the s -channel nature of this process. As long as we are only concerned with the h_c energy distribution, one can reexpress the h_c production rate from e^+e^- annihilation in terms of that from virtual photon decay [42]:

$$d\sigma [e^+e^- \rightarrow h_c + X] = \frac{4\pi\alpha}{s^{3/2}} d\Gamma [\gamma^* \rightarrow h_c + X], \quad (4)$$

¹ It was first made clear by Nayak, Qiu and Sterman [39, 40] a decade ago that the original definition of the NRQCD color-octet production operator [9] is not gauge invariant, and the correct definition necessitates the inclusion of eikonal lines that run from the quark/antiquark field to infinity. To the perturbative order considered in this work, this nuisance does not play a role so we can stick to the conventional definition.

where the center-of-mass energy of the e^+e^- system is denoted by \sqrt{s} .

Some representative Feynman diagrams for the $c\bar{c}(n)$ production from e^+e^- annihilation in both color-singlet and color octet channels are shown in Fig. 1. Due to the odd C parity of the h_c meson, the color-singlet channel starts at $\mathcal{O}(\alpha_s^2)$, while the octet contribution starts at $\mathcal{O}(\alpha_s)$. In the rest of this section, we will briefly review the LO results for F_8 and F_1 , which were first analytically computed in Ref. [19].

B. LO SDC in the color-octet channel

At LO in color-octet channel, we only need consider $e^+e^- \rightarrow c\bar{c}(^1S_0^{(8)}) + g$. The differential two-body phase space in d dimensions reads [19]

$$d\Phi_2 = \frac{c_\epsilon}{8\pi} s^{-\epsilon} (1-r)^{1-2\epsilon} \delta(1+r-z) dz, \quad (5)$$

where $c_\epsilon \equiv (4\pi)^\epsilon \frac{\Gamma(1-\epsilon)}{\Gamma(2-2\epsilon)}$. $r \equiv 4m_c^2/s$ is introduced for notational convenience. For future use, we also define the energy fraction variable $z \equiv 2P^0/\sqrt{s}$, where $P^\mu = (P^0, \mathbf{P})$ represents the four-momentum of the $c\bar{c}$ pair.

The LO squared quark amplitude turns to be

$$\sum_{\text{Pol,Col}} \left| \mathcal{M}_0 \left[\gamma^* \rightarrow c\bar{c} \left(^1S_0^{(8)} \right) + g \right] \right|^2 = 256\pi^2 e_c^2 \alpha C_A C_F \alpha_s \mu^{2\epsilon} (1-\epsilon)(1-2\epsilon), \quad (6)$$

where $e_c = \frac{2}{3}$ is the electric charge of the charm quark, $C_A = 3$ and $C_F = \frac{4}{3}$ are color Casimirs. Integrating (6) over the two-body phase space in (5), we obtain

$$\begin{aligned} \hat{\sigma}_0^{(8)} &\equiv \frac{2\pi\alpha}{3s^2} \int d\Phi_2 \left| \mathcal{M}_0 \left[\gamma^* \rightarrow c\bar{c} \left(^1S_0^{(8)} \right) + g \right] \right|^2 \\ &= \frac{64\pi^2 e_c^2 \alpha^2 C_A C_F \alpha_s (1-r)^{1-2\epsilon}}{3s^2} \left(\frac{4\pi\mu^2}{s} \right)^\epsilon \frac{\Gamma(2-\epsilon)}{\Gamma(1-2\epsilon)}. \end{aligned} \quad (7)$$

The factor $\frac{1}{3}$ accounts for averaging over three polarizations of γ^* .

Comparing both sides of (1) for the color-octet channel, taking the $d \rightarrow 4$ limit, we then deduce the LO SDC accordingly:

$$\frac{dF_8^{\text{LO}}}{dz} = \frac{32\pi^2 e_c^2 \alpha^2 \alpha_s m_c}{3s^2} (1-r) \delta(1+r-z), \quad (8)$$

In the high energy limit, the integrated SDC reads

$$F_8^{\text{LO}} \Big|_{\sqrt{s} \gg m_c} = \frac{32\pi^2 e_c^2 \alpha^2 \alpha_s m_c}{3s^2}. \quad (9)$$

C. LO SDC in the color-singlet channel

To determine the LO SDC in the color-singlet channel, we need consider $e^+e^- \rightarrow c\bar{c}(^1P_1^{(1)}) + gg$. The IR divergence appears in the upper endpoint of the h_c spectrum, when

one of the gluons becomes soft, which is handled by DR [19]. Finally, as a virtue of the famous color-octet mechanism of NRQCD, the single IR pole is factored into the color-octet LDME. As a remnant of this IR divergence, the SDC F_1 acquires a logarithmical dependence on the NRQCD factorization scale μ_Λ . The differential SDC dF_1/dz is somewhat too lengthy to be reproduced here, and we refer the interested readers to Ref. [19] for more details. Here we just list the integrated color-singlet short-distance coefficient:

$$F_1^{\text{LO}}(\mu_\Lambda)_{\overline{\text{MS}}} = \frac{64\pi e_c^2 \alpha^2 C_F \alpha_s^2 m_c}{9N_c s^2} (1-r) \left[-\ln \frac{\mu_\Lambda^2}{4m_c^2} + 2\ln(1-r) + \frac{7+7r-9r^2}{6(1-r)^2} \ln r \right. \\ \left. + \frac{r(5-7r)}{16(1-r)^2} \ln^2 \frac{1+\sqrt{1-r}}{1-\sqrt{1-r}} - \frac{65-84r}{12(1-r)} + \frac{14-15r}{8(1-r)^{3/2}} \ln \frac{1+\sqrt{1-r}}{1-\sqrt{1-r}} \right]. \quad (10)$$

It is enlightening to see the asymptotic behavior of F_1^{LO} in the limit high energy limit:

$$F_1^{\text{LO}}(\mu_\Lambda)_{\overline{\text{MS}}} \Big|_{\sqrt{s} \gg m_c} \rightarrow \frac{64\pi e_c^2 \alpha^2 C_F \alpha_s^2 m_c}{9N_c s^2} \left(-\frac{7}{12} \ln r - \ln \frac{\mu_\Lambda^2}{4m_c^2} - \frac{65}{12} + \frac{7}{2} \ln 2 \right). \quad (11)$$

Note the occurrence of the $\ln r$ inside the bracket is linear.

III. ORDER- α_s CORRECTION TO THE COLOR-OCTET CHANNEL

In this Section, we are going to calculate the NLO radiative corrections to the color-octet SDC short-distance coefficient dF_8 . The NLO corrections include the real correction $e^+e^- \rightarrow c\bar{c}(^1S_0^{(8)}) + gg(q\bar{q})$ together with the one-loop virtual correction to $e^+e^- \rightarrow c\bar{c}(^1S_0^{(8)}) + g$. The UV divergence appearing in the virtual correction would be removed by the renormalization program, while the IR singularities would cancel away when summing both real and virtual corrections.

During this work, we generate the decay amplitudes using the ppackage **FeynArts** [43], and employ the the package **FeynCalc** [44] to conduct the contraction of Lorentz indices and traces over the Dirac matrices.

We note that the NLO correction to $e^+e^- \rightarrow c\bar{c}(^1S_0^{(8)}) + gg$ has already been computed by Zhang et al. [45] about a decade ago. Nevertheless, those authors employed a purely numerical recipe, and our goal is instead to present fully analytical results for the SDCs. Our final numerical result agrees with what is given in Ref. [45].

A. Real corrections

There are more Feynman diagrams for $e^+e^- \rightarrow c\bar{c}(^1S_0^{(8)}) + gg(q\bar{q})$ than the color-singlet channel, due to color-octet feature of the $c\bar{c}$ pair. One of the real-emission diagrams is shown in Fig. 1. In this section, we will briefly explain how we derive the analytic results by integrating the squared amplitudes over the three-body phase space in DR, closely following the recipe outlined in Ref. [19]. Some specific technical details are presented in Appendix A. To ensure the correctness of our results, we also redo the calculation numerically, utilizing the two-cutoff phase space slicing method [46], and find the full agreement.

First, we introduce two additional fractional energy variables x_1 and x_2 besides z :

$$x_1 \equiv \frac{2k_1^0}{\sqrt{s}}, \quad x_2 \equiv \frac{2k_2^0}{\sqrt{s}}, \quad (12)$$

where k_1 and k_2 represent the momenta of the final-state gluons (light quarks) in real emission process. These variables are subject to the constraint $x_1 + x_2 + z = 2$, by energy conservation. For convenience, we separate the squared amplitude for $\gamma^* \rightarrow c\bar{c} \left({}^1S_0^{(8)} \right) + gg$ into four pieces:

$$\sum_{\text{Pol,Col}} \left| \mathcal{M} \left[\gamma^* \rightarrow c\bar{c} \left({}^1S_0^{(8)} \right) + gg \right] \right|^2 = \mathcal{I}_{\text{SC}}(x_i, z) + \mathcal{I}_{\text{S}}(x_i, z) + \mathcal{I}_{\text{C}}(x_i, z) + \mathcal{I}_{\text{Fin}}(x_i, z). \quad (13)$$

The first term $\mathcal{I}_{\text{SC}}(x_i, z)$ would potentially yield both soft and collinear divergences upon phase-space integration. The second term $\mathcal{I}_{\text{S}}(x_i, z)$ would potentially yield only soft singularity upon integration, when one of the gluon becomes soft. The third term $\mathcal{I}_{\text{C}}(x_i, z)$ would potentially generate collinear singularity only, when two gluons become collinear to each other. The last term \mathcal{I}_{Fin} will not lead to any divergences, so we can perform the phase space integration in 4 dimensions. These integrands explicitly read

$$\mathcal{I}_{\text{SC}} = - \frac{2^{12} \pi^3 e_c^2 \alpha C_A^2 C_F \alpha_s^2 \mu^{4\epsilon} (1-\epsilon)(1-2\epsilon)(1-r)}{s} \frac{1}{1+r-z} \left(\frac{1}{1+r-z-x_1} + \frac{1}{1+r-z-x_2} \right), \quad (14a)$$

$$\mathcal{I}_{\text{S}} = - \frac{2^{12} \pi^3 e_c^2 \alpha C_A^2 C_F \alpha_s^2 \mu^{4\epsilon} (1-\epsilon)(1-2\epsilon)r}{s} \left[\frac{1}{(1+r-z-x_1)^2} + \frac{1}{(1+r-z-x_2)^2} \right], \quad (14b)$$

$$\mathcal{I}_{\text{C}} = - \frac{2^{12} \pi^3 e_c^2 \alpha C_A^2 C_F \alpha_s^2 \mu^{4\epsilon} (1-\epsilon)(1-2\epsilon) 2(1-r)^2 - x_1(1-r-x_1)}{(1-r)^2 s} \frac{1}{1+r-z}. \quad (14c)$$

$$\begin{aligned} \mathcal{I}_{\text{Fin}} = & \frac{2^{12} \pi^3 e_c^2 \alpha C_A^2 C_F \alpha_s^2}{(1-r)^2 (2-z)^2 (1-r-x_1)^2 (1+r-z-x_1)^2 s} \left\{ x_1^6 (3-r-z) \right. \\ & + x_1^5 (2-z)(3r+2z-7) - x_1^4 (2-z)^2 (5r+z-7) + (1-r)x_1^3 (2-z)^2 (2r+3z-8) \\ & - (1-r)^2 x_1^2 [r^3 - r^2(z-1) + r(z^2 - 4z + 3) + 2z^3 - 13z^2 + 29z - 21] \\ & + (1-r)^2 x_1 (2-z) [r^3 + r^2(3-2z) + r(3z^2 - 10z + 7) - z^3 + 3z^2 - 3] \\ & \left. + (1-r)^3 (2-z)^2 (1+r-z)(z-2r) \right\}. \end{aligned} \quad (14d)$$

Integrating (13) over the three-body phase space, we have

$$\hat{\sigma}_{\text{R}}^{(8),gg} \equiv \hat{\sigma}_{\text{Div}}^{(8),gg} + \hat{\sigma}_{\text{Fin}}^{(8),gg} = \frac{1}{2!} \frac{2\pi\alpha}{3s^2} \int d\Phi_3 (\mathcal{I}_{\text{SC}} + \mathcal{I}_{\text{S}} + \mathcal{I}_{\text{C}} + \mathcal{I}_{\text{Fin}}), \quad (15)$$

where $d\Phi_3$ signifies the differential three-body phase space as shown in Eq. (A.1). We have also included a factor $\frac{1}{2!}$ to account for the indistinguishability of final-state gluons. Concretely, the “divergent” and “finite” pieces in (15) are defined by

$$\hat{\sigma}_{\text{Div}}^{(8),gg} = \int_{2\sqrt{r}}^{1+r} dz \frac{d\hat{\sigma}_{\text{Div}}^{(8),gg}}{dz} = \frac{1}{2!} \frac{2\pi\alpha}{3s^2} \int d\Phi_3 (\mathcal{I}_{\text{SC}} + \mathcal{I}_{\text{S}} + \mathcal{I}_{\text{C}}), \quad (16a)$$

$$\hat{\sigma}_{\text{Fin}}^{(8),gg} = \int_{2\sqrt{r}}^{1+r} dz \frac{d\hat{\sigma}_{\text{Fin}}^{(8),gg}}{dz} = \frac{1}{2!} \frac{2\pi\alpha}{3s^2} \int d\Phi_3 \mathcal{I}_{\text{Fin}}. \quad (16b)$$

After integrating the squared amplitudes over x_1 in (16), we then arrive at the following energy distribution:

$$\begin{aligned} \frac{d\hat{\sigma}_{\text{Div}}^{(8),gg}}{dz} = & \hat{\sigma}_0^{(8)} \frac{\alpha_s}{\pi} \frac{(1-r)^{-2\epsilon} r^\epsilon}{\Gamma(1-\epsilon)} \left(\frac{4\pi\mu^2}{s} \right)^\epsilon \\ & \times C_A \left\{ \frac{1}{2} \left(\frac{1}{\epsilon^2} + \frac{17}{6} \frac{1}{\epsilon} - 4 \ln^2 \frac{\sqrt{r}}{1+\sqrt{r}} - \frac{23}{3} \ln \frac{\sqrt{r}}{1+\sqrt{r}} - \frac{\pi^2}{2} + \frac{67}{18} \right) \delta(1+r-z) \right. \\ & + \left[\frac{1}{1+r-z} \right]_+ \left[2 \ln \frac{2-z+\sqrt{z^2-4r}}{2} - \ln \frac{z-\sqrt{z^2-4r}}{z+\sqrt{z^2-4r}} \right. \\ & \left. \left. - \frac{2\sqrt{z^2-4r}}{1-r} - \frac{\sqrt{z^2-4r}(2z^2-3z-3rz+4r)}{12(1-r)^3} \right] - \left[\frac{\ln(1+r-z)}{1+r-z} \right]_+ \right\}, \end{aligned} \quad (17a)$$

$$\begin{aligned} \frac{d\hat{\sigma}_{\text{Fin}}^{(8),gg}}{dz} = & \hat{\sigma}_0^{(8)} \frac{\alpha_s}{\pi} \frac{C_A}{12(1-r)^3(z-2r)^3(2-z)^2} \left\{ \sqrt{z^2-4r} [144r^6 - 8r^5(27z+56) \right. \\ & + 8r^4(11z^2+94z+48) + 4r^3(4z^3-111z^2-168z-12) \\ & - r^2(30z^4-170z^3-216z^2-360z+144) + r(13z^5-58z^4+36z^3-204z^2+24z+48) \\ & \left. - z(2z^5-9z^4+12z^3-18z^2-24z+24)] \right. \\ & - 12(1-r)^2 \ln \frac{z-2r-\sqrt{z^2-4r}}{z-2r+\sqrt{z^2-4r}} [12r^5-8r^4(3z+1)+8r^3(3z^2-z+3) \\ & \left. - r^2(16z^3-30z^2+48z-8) + 2r(3z^4-9z^3+12z^2-2) - z^2(z^3-4z^2+6z-2)] \right\}, \end{aligned} \quad (17b)$$

where the “+”-function is defined as

$$\int_{2\sqrt{r}}^{1+r} dz [f(z)]_+ g(z) = \int_{2\sqrt{r}}^{1+r} dz f(z) [g(z) - g(1+r)], \quad (18)$$

where $g(z)$ is a smooth test function.

Note the occurrence of the double IR poles in (17a), reflecting the simultaneous emergence of the soft and collinear singularities right sitting in the endpoint $z = 1+r$.

Integrating Eq. (17) over z , we then obtain the integrated real emission cross section:

$$\begin{aligned} \hat{\sigma}_R^{(8),gg} = & \hat{\sigma}_0^{(8)} \frac{\alpha_s}{\pi} \frac{(1-r)^{-2\epsilon} r^\epsilon}{\Gamma(1-\epsilon)} \left(\frac{4\pi\mu^2}{s} \right)^\epsilon \frac{C_A}{2} \left[\frac{1}{\epsilon^2} + \frac{17}{6} \frac{1}{\epsilon} + \frac{2-3r}{8(1-r)} \ln^2 \frac{1-\sqrt{1-r}}{1+\sqrt{1-r}} \right. \\ & \left. + \frac{10-9r}{6(1-r)^{3/2}} \ln \frac{1-\sqrt{1-r}}{1+\sqrt{1-r}} + 2\text{Li}_2(r) - \ln^2 r + 2 \ln r \ln(1-r) + \frac{1-6 \ln r}{3(1-r)} + \frac{235}{18} - \frac{7\pi^2}{6} \right]. \end{aligned} \quad (19)$$

Likewise, we can carry out the similar manipulation for the process $\gamma^* \rightarrow c\bar{c}({}^1S_0^{(8)}) + q\bar{q}$. The squared amplitude in d dimensions is

$$\begin{aligned} \sum_{u,d,s} \sum_{\text{Pol,Col}} \left| \mathcal{A} \left[\gamma^* \rightarrow c\bar{c}({}^1S_0^{(8)}) + q\bar{q} \right] \right|^2 = & \frac{2^{10}\pi^3 e_c^2 \alpha C_A C_F n_f \alpha_s^2 \mu^{4\epsilon} (1-2\epsilon)}{(2-z)^2(1+r-z)s} \\ & \times [2x_1^2 - 2(2-z)x_1 + z^2(1-\epsilon) - 2z + 2 - 2r(1-2\epsilon)], \end{aligned} \quad (20)$$

where $n_f = 3$ represents the inclusion of three light flavors u , d and s . After integrating (20) over the the three-body phase space integral in (A.1), we find

$$\begin{aligned} \frac{d\hat{\sigma}_R^{(8),q\bar{q}}}{dz} = & \hat{\sigma}_0^{(8)} \frac{\alpha_s}{\pi} \frac{(1-r)^{-2\epsilon} r^\epsilon}{\Gamma(1-\epsilon)} \left(\frac{4\pi\mu^2}{s} \right)^\epsilon \frac{n_f}{6} \left\{ \left[-\frac{1}{\epsilon} + 2 \ln \frac{\sqrt{r}}{1+\sqrt{r}} - \frac{5}{3} \right] \delta(1+r-z) \right. \\ & \left. + \left[\frac{1}{1+r-z} \right]_+ \frac{(z^2-4r)^{3/2}}{(1-r)(2-z)^2} \right\}. \end{aligned} \quad (21)$$

Unlike the case for $\hat{\sigma}_R^{(8),gg}$, here only the single IR pole is present, indicating only the collinear singularity arises in the $c\bar{c}(^1S_0^{(8)}) + q\bar{q}$ channel.

The integrated real emission cross section in $q\bar{q}$ channel is

$$\hat{\sigma}_R^{(8),q\bar{q}} = \hat{\sigma}_0^{(8)} \frac{\alpha_s}{\pi} \frac{(1-r)^{-2\epsilon} r^\epsilon}{\Gamma(1-\epsilon)} \left(\frac{4\pi\mu^2}{s} \right)^\epsilon \frac{n_f}{6} \left(-\frac{1}{\epsilon} - \frac{20-8r-9\ln r}{3(1-r)} - \frac{2}{(1-r)^{3/2}} \ln \frac{1-\sqrt{1-r}}{1+\sqrt{1-r}} \right). \quad (22)$$

B. Virtual corrections

To render finite predictions, the IR singularities encoded in Eq. (17) and (21) encounter in the real corrections should be canceled by including the one-loop virtual corrections. One typical one-loop diagram for $e^+e^- \rightarrow c\bar{c}(^1S_0^{(8)}) + g$ is shown in Fig. 1. Upon including the quark mass and QCD coupling constant renormalization, and with the aid of LSZ reduction formula, the UV divergences in the virtual correction amplitude will be eliminated.

Upon calculating the loop diagrams, the partial fraction of the integrand is performed with the aid of the the package **\$Apart** [47] and the integration-by-part reduction is facilitated by the package **FIRE** [48]. The resulting master integrals are calculated analytically, against which are checked numerically by the package **LoopTools** [49].

After squaring the amplitudes and integration over the two-body phase space, we obtain

$$\hat{\sigma}_V^{(8)} \equiv \frac{2\pi\alpha}{3s^2} \int d\Phi_2 2\text{Re} \left\{ \mathcal{M}_0 \left[\gamma^* \rightarrow c\bar{c} (^1S_0^{(8)}) + g \right] \mathcal{M}_1^* \left[\gamma^* \rightarrow c\bar{c} (^1S_0^{(8)}) + g \right] \right\}, \quad (23)$$

where \mathcal{M}_1 denotes the renormalized one-loop QCD amplitude, which can be readily computed in an analytic fashion. After some manipulation, we can deduce the differential cross section from the virtual correction:

$$\begin{aligned} \frac{d\hat{\sigma}_V^{(8)}}{dz} = & \hat{\sigma}_0^{(8)} \frac{\alpha_s}{\pi} \frac{(1-r)^{-2\epsilon} r^\epsilon}{\Gamma(1-\epsilon)} \left(\frac{4\pi\mu^2}{s} \right)^\epsilon \frac{1}{2} \left\{ -\frac{C_A}{\epsilon^2} - \frac{2C_A + \beta_0}{2\epsilon} + \frac{\beta_0}{2} \ln \frac{\mu^2}{m_c^2} \right. \\ & + \frac{C_A(2-r) - 2C_F(2+r)}{4(1-r)} \ln^2 \frac{1-\sqrt{1-r}}{1+\sqrt{1-r}} + \frac{3(C_A - 2C_F)}{\sqrt{1-r}} \ln \frac{1-\sqrt{1-r}}{1+\sqrt{1-r}} \\ & + \frac{C_A(1-r) + 2C_F}{2(1-r)} \left(\ln^2 \frac{r}{2-r} + 2\text{Li}_2 \frac{r}{2-r} \right) \\ & + \frac{-2C_A(2-r) + 4C_F(3-2r) + (2-r)^2\beta_0}{(2-r)^2} \ln \frac{r}{2(1-r)} + \frac{C_A(9+4\pi^2)}{3} \\ & \left. - \frac{C_F[\pi^2(2-r) + 6(1-r)(9-5r)]}{3(2-r)(1-r)} \right\} \delta(1+r-z), \end{aligned} \quad (24)$$

where $\beta_0 = \frac{11}{3}C_A - \frac{2}{3}n_f$ is the one-loop coefficient of the QCD β -function. Note here the $1/\epsilon$ poles are purely of infrared origin.

C. Adding real and virtual corrections

It is time to sum up the real corrections from the $gg/q\bar{q}$ channels, which are encoded in (17) and (21), and the virtual correction (24). As anticipated, all the double and single IR poles cancel, and we end up with the following differential cross section:

$$\begin{aligned}
\frac{d\hat{\sigma}^{(8)}}{dz} = & \sigma_0^{(8)} \frac{\alpha_s}{\pi} \left\{ \frac{\beta_0}{4} \ln \frac{\mu^2}{m_c^2} + \frac{C_A(2-r) - 2C_F(2+r)}{8(1-r)} \ln^2 \frac{1-\sqrt{1-r}}{1+\sqrt{1-r}} + \frac{3(C_A - 2C_F)}{2\sqrt{1-r}} \ln \frac{1-\sqrt{1-r}}{1+\sqrt{1-r}} \right. \\
& + \frac{C_A(1-r) + 2C_F}{4(1-r)} \left(\ln^2 \frac{r}{2-r} + 2\text{Li}_2 \frac{r}{2-r} \right) + \frac{-2C_A(2-r) + 4C_F(3-2r) + (2-r)^2\beta_0}{2(2-r)^2} \ln \frac{r}{2(1-r)} \\
& - \frac{C_F[\pi^2(2-r) + 6(1-r)(9-5r)]}{6(2-r)(1-r)} - 2C_A \ln^2 \frac{\sqrt{r}}{1+\sqrt{r}} + \frac{-23C_A + 2n_f}{6} \ln \frac{\sqrt{r}}{1+\sqrt{r}} \\
& \left. + \frac{121C_A + 15\pi^2C_A - 10n_f}{36} \right\} \delta(1+r-z) \\
& + \sigma_0^{(8)} \frac{\alpha_s}{\pi} \left\{ \left[\frac{1}{1+r-z} \right]_+ C_A \left[2 \ln \frac{2-z+\sqrt{z^2-4r}}{2} - \ln \frac{z-\sqrt{z^2-4r}}{z+\sqrt{z^2-4r}} - \frac{2\sqrt{z^2-4r}}{1-r} \right. \right. \\
& \left. \left. - \frac{\sqrt{z^2-4r}(2z^2-3z-3rz+4r)}{12(1-r)^3} \right] - C_A \left[\frac{\ln(1+r-z)}{1+r-z} \right]_+ + \left[\frac{1}{1+r-z} \right]_+ \frac{n_f}{6} \frac{(z^2-4r)^{3/2}}{(1-r)(2-z)^2} \right\} \\
& + \hat{\sigma}_0^{(8)} \frac{\alpha_s}{\pi} \frac{C_A}{12(1-r)^3(z-2r)^3(2-z)^2} \left\{ \sqrt{z^2-4r} [144r^6 - 8r^5(27z+56) \right. \\
& + 8r^4(11z^2+94z+48) + 4r^3(4z^3-111z^2-168z-12) \\
& - r^2(30z^4-170z^3-216z^2-360z+144) + r(13z^5-58z^4+36z^3-204z^2+24z+48) \\
& \left. - z(2z^5-9z^4+12z^3-18z^2-24z+24) \right] \\
& - 12(1-r)^2 \ln \frac{z-2r-\sqrt{z^2-4r}}{z-2r+\sqrt{z^2-4r}} [12r^5-8r^4(3z+1)+8r^3(3z^2-z+3) \\
& \left. - r^2(16z^3-30z^2+48z-8) + 2r(3z^4-9z^3+12z^2-2) - z^2(z^3-4z^2+6z-2) \right] \left. \right\}. \tag{25}
\end{aligned}$$

After integrating (25) over z , we then get the integrated SDC F_8^{NLO} at NLO in α_s :

$$\begin{aligned}
F_8^{\text{NLO}} = F_8^{\text{LO}} + F_8^{\text{LO}} \frac{\alpha_s}{\pi} & \left\{ \frac{\beta_0}{4} \ln \frac{\mu^2}{m_c^2} + \frac{C_A(6-5r) - 4C_F(2+r)}{16(1-r)} \ln^2 \frac{1-\sqrt{1-r}}{1+\sqrt{1-r}} \right. \\
& + \frac{C_A(28-27r) - 36C_F(1-r) - 4n_f}{12(1-r)^{3/2}} \ln \frac{1-\sqrt{1-r}}{1+\sqrt{1-r}} + \frac{C_A}{2} [2\text{Li}_2 r - \ln^2 r + 2 \ln r \ln(1-r)] \\
& + \frac{C_A(1-r) + 2C_F}{4(1-r)} \left(\ln^2 \frac{r}{2-r} + 2\text{Li}_2 \frac{r}{2-r} \right) + \frac{C_A(1-6 \ln r)}{6(1-r)} - \frac{n_f(20-8r-9 \ln r)}{18(1-r)} \\
& + \frac{-2C_A(2-r) + 4C_F(3-2r) + (2-r)^2 \beta_0}{2(2-r)^2} \ln \frac{r}{2(1-r)} \\
& \left. - \frac{C_F[\pi^2(2-r) + 6(1-r)(9-5r)]}{6(2-r)(1-r)} + \frac{C_A(289+3\pi^2)}{36} \right\}. \tag{26}
\end{aligned}$$

As mentioned before, the numerical value of F_8^{NLO} in Eq. (26) was also obtained in Ref. [45]. When taking their input parameters, our result is consistent with theirs.

In the $\sqrt{s} \gg m_c$ limit, the integrated SDC F_8^{NLO} assumes the following asymptotic form:

$$\begin{aligned}
F_8^{\text{NLO}} \Big|_{\text{Asym}} = F_8^{\text{LO}} + F_8^{\text{LO}} \frac{\alpha_s}{\pi} & \left[\frac{\beta_0}{4} \ln \frac{\mu^2}{m_c^2} + \frac{C_A}{8} \ln^2 r - (2C_A - C_F) \ln 2 \ln r \right. \\
& + \frac{16C_A - 9C_F - n_f}{6} \ln r + \frac{7C_A - 6C_F}{4} \ln^2 2 - \frac{12C_A - 9C_F - 2n_f}{2} \ln 2 \\
& \left. + \frac{295C_A - 162C_F - 40n_f + 3(C_A - 2C_F)\pi^2}{36} \right]. \tag{27}
\end{aligned}$$

In contrast to $F_1|_{\text{asym}}$, a double logarithm $\ln^2 r$ has arisen.

From Eqs. (11) and (27), one see that in the asymptotic limit,

$$F_1^{\text{LO}} \sim -\frac{\alpha_s^2}{s^2} \ln r, \quad F_8^{\text{NLO}} - F_8^{\text{LO}} \sim \frac{\alpha_s^2}{s^2} \ln^2 r. \tag{28}$$

Since $\ln^2 r \gg |\ln r|$ asymptotically, this result may indicate that the color-octet channel dominates the inclusive h_c production rate over the color-singlet one, at sufficiently high energy. The occurrence of $\ln^2 r$ at NLO strongly suggests that, it appears to be desirable to resum these types of double logarithms to all orders in α_s in the color-octet channel. We believe the appropriate formalism to achieve this goal is the double-parton fragmentation approach [50–52].

IV. END-POINT RESUMMATION FOR COLOR OCTET CHANNEL

When we reach the end-point region in which $z \rightarrow 1+r$ and the h_c carries its maximally allowed energy, fixed order calculations are plagued with large threshold logarithms of the form $\sum_{j < i} \alpha_s^i [\log^{2i-j}(1+r-z)/(1+r-z)]_+$. To provide reliable predictions, these threshold logarithms have to be resummed to all orders. In this section we resum those logarithms to the next-to-leading-logarithmic (NLL) accuracy within the SCET framework [33–38].

Following Ref. [32], the factorization theorem for the color octet h_c production is found to take the form

$$\frac{d\sigma}{dz'} = \hat{\sigma}_0^{(8)} H[\mu_H, \mu] \int_{z'}^1 dx S[x, \mu_S, \mu] \times J[s(1+r)(x-z'), \mu_J, \mu], \tag{29}$$

where we have introduced

$$z' = \frac{E_{h_c}}{E_{h_c}^{\max}} = \frac{z}{1+r}. \quad (30)$$

Here H is the hard function normalized to 1. The hard function which encodes the virtual corrections can be calculated perturbatively. Its one-loop results and anomalous dimension γ_H can be extracted from Eq. (24). S and J stand for the shape and jet functions, respectively.

The shape function $S^{(8,^1S_0)}(\ell^+)$ is defined in terms of ultrasoft fields that carry $\mathcal{O}(\Lambda_{\text{QCD}})$ momentum

$$S(\ell^+) = \frac{\langle 0 | \chi^\dagger T^A \psi a_{h_c}^\dagger a_{h_c} \delta(\ell^+ - in \cdot D) \psi^\dagger T^A \chi | 0 \rangle}{4m_c \langle \mathcal{O}_8^{h_c} (^1S_0) \rangle}, \quad (31)$$

where the ultrasoft covariant derivative can be written as $D^\mu = \partial^\mu - ig_s A_{us}^\mu$ and the lightlike vectors are defined as $n^\mu = (1, 0, 0, -1)$ and $\bar{n}^\mu = (1, 0, 0, 1)$. χ and ψ are the heavy quark fields to create a heavy quark and antiquark defined previously while $a_{h_c}^\dagger a_{h_c}$ is the projector to project onto the final h_c state. The normalizations of the shape function is written as $\int d\ell^+ S(\ell^+) = 1$.

The jet function describes the collinear radiations recoil against the h_c in the threshold region. The jet function is independent of the state of the charm quark-antiquark pair and is defined as

$$J(\bar{n} \cdot pn \cdot k + p_\perp^2) = -\frac{s(1+r)}{4\pi} \text{Im} s[i \int d^4 y e^{ik \cdot y} \langle 0 | T \{ \text{Tr}[T^A B_\perp^{(0)\beta}(y)] \text{Tr}[T^A B_{\perp\beta}^{(0)}(0)] \} | 0 \rangle], \quad (32)$$

where the subscript \perp denotes the perpendicular direction, the superscript (0) denotes the bare field, and B_\perp^μ is the collinear gauge invariant effective field which can be written as

$$B_\perp^\mu = \frac{1}{g_s} W^\dagger (\mathcal{P}_\perp^\mu + g_s (A_{n,q}^\mu)_\perp) W, \quad (33)$$

with a collinear gluon field $A_{n,q}^\mu$ and a collinear Wilson line $W_n(x) = \sum_{\text{perms}} \text{Exp}(-g_s \frac{1}{\mathcal{P}} \bar{n} \cdot A_{n,q}(x))$. Here \mathcal{P} is the projection operator which picks out the large component of the momenta to its right [34].

The one-loop anomalous dimension γ_J for the jet function can be found in Ref. [32], while the anomalous dimension for the soft function can be inferred from the consistency condition $\gamma_S + \gamma_H + \gamma_J = 0$.

To resum the large end-point logarithms, all components H , J and S in the factorization theorem will be evolved from their natural scales μ_H , μ_J and μ_S to a common scale μ to evaluate the cross section, following the renormalization group (RG) equation

$$\frac{dF_i}{d \log \mu} = \gamma_i F_i, \quad (34)$$

where i runs over the hard (H), collinear (J) and the soft (S) modes. The scales μ_H , μ_J and μ_S set the initial condition for the RG running and are chosen to minimize the logarithms in the higher order corrections to H , J and S , respectively, which is found to be of order

$$\begin{aligned} \mu_H &\sim \frac{s}{M}(1-r), & \mu_S &\sim M \frac{1+r}{1-r}(1-z'), \\ \mu_J &\sim \sqrt{\mu_H \mu_S}, \end{aligned} \quad (35)$$

where we have set $M = 2m_c$. After combining all pieces and assuming $\mu_J = \sqrt{\mu_H \mu_S}$, we arrived at a compact form for the NLL cross section, which reads

$$\frac{d\sigma_{\text{pert.}}^{\text{NLL}}}{dz'} = \sigma_0^{(8)} e^h \left[\frac{\mu_H M}{s(1-r)} \right]^{2C_A A_\gamma[\mu_H, \mu_J]} \left[\frac{\mu_S}{M} \frac{1-r}{1+r} \right]^\omega \frac{e^{\omega \gamma_E}}{\Gamma[1-\omega]} (1-z')^{-\omega}, \quad (36)$$

where γ_E is the Euler constant and we define the auxiliary parameters

$$\begin{aligned} h &= 2C_A \bar{S}(\mu_H, \mu) - A_H(\mu_H, \mu) + 2C_A \bar{S}(\mu_S, \mu) - A_S(\mu_S, \mu) - 4C_A \bar{S}(\mu_J, \mu) - A_J(\mu_J, \mu), \\ \omega &= 2C_A A_\gamma[\mu_S, \mu_J] < 0, \end{aligned} \quad (37)$$

and \bar{S} and A_i are found to be

$$\bar{S}(\mu_i, \mu_f) = \left[\frac{4\pi}{\alpha_s(\mu_i)} \left(1 - \frac{1}{\rho} - \log \rho \right) + \frac{\beta_1}{2\beta_0} \log^2 \rho + (1 - \rho + \log \rho) \left(\frac{\gamma_1}{\gamma_0} - \frac{\beta_1}{\beta_0} \right) \right] \frac{\gamma_0}{4\beta_0^2} \quad (38a)$$

$$A_\gamma(\mu_i, \mu_f) = \frac{\gamma_0}{2\beta_0} \left[\log \rho + \frac{\alpha_s(\mu_i)}{4\pi} \left(\frac{\gamma_1}{\gamma_0} - \frac{\beta_1}{\beta_0} \right) (\rho - 1) \right], \quad (38b)$$

where

$$\rho = \frac{\alpha_s(\mu_f)}{\alpha_s(\mu_i)}, \quad (39a)$$

$$\beta_0 = \frac{11}{3} C_A - \frac{2}{3} n_f, \quad (39b)$$

$$\beta_1 = \frac{34}{3} C_A^2 - \frac{20}{3} C_A T_F n_f - 4 C_F T_F n_f, \quad (39c)$$

$$\gamma_0 = 4, \quad \gamma_1 = \left(\frac{67}{9} - \frac{\pi^2}{3} \right) C_A - \frac{20}{9} T_F n_f. \quad (39d)$$

Up to NLL accuracy, A_H , A_J and A_S are obtained by truncating out the α_s term and replacing γ_0 in A_γ with γ_0^H , γ_0^J or γ_0^S with

$$\begin{aligned} \gamma_0^H &= -\frac{34}{3} C_A + \frac{4}{3} n_f, & \gamma_0^J &= 2\beta_0, \\ \gamma_0^S &= -\gamma_0^H - \gamma_0^J = 4C_A. \end{aligned} \quad (40)$$

Last we note that when $(1-z') \sim \mathcal{O}(\Lambda_{\text{QCD}}/M)$, the process-independent shape function becomes non-perturbative and therefore a non-perturbative model $\mathcal{S}_{\text{non-pert.}}$ is required for describing the non-perturbative soft radiations and the resummed cross section is modified as

$$\frac{d\sigma^{\text{NLL}}}{dz'} = \int_{z'}^1 \frac{dx}{x} \frac{d\sigma_{\text{pert.}}^{\text{NLL}}}{dx} \mathcal{S}_{\text{non-pert.}} \left(\frac{z'}{x} \right), \quad (41)$$

where the non-perturbative shape function is adopted by a modified version of a model used in the decay of B mesons [53]

$$\mathcal{S}_{\text{non-pert.}}(\ell^+) = \frac{1}{\bar{\Lambda}} \frac{a^{ab}}{\Gamma(ab)} (x-1)^{ab-1} e^{-a(x-1)}, \quad (42)$$

with $x = \ell^+/\bar{\Lambda}$ and $\bar{\Lambda} = m_{h_c} - 2m_c$.

Refs.	$\langle \mathcal{O}_8^{h_c(1P)}(^1S_0) \rangle$	$\sigma_{\text{LO}}^{(1)}$	$\sigma_{\text{LO}}^{(8)}$	$\sigma_{\text{NLO}}^{(8)}$	$\sigma_{\text{LO}}^{(1)} + \sigma_{\text{NLO}}^{(8)}$
[54, 55]	0.007		72.41	135.21	124.62
[56]	0.0098	-10.59	101.38	189.29	178.70
[57]	0.016		165.52	309.04	298.46

Table I: Numeric results for the total cross sections(fb). To show the dependence of the cross sections on the color octet LDMEs, we list different results by varying the value of $\langle \mathcal{O}_8^{h_c(1P)}(^1S_0) \rangle$.

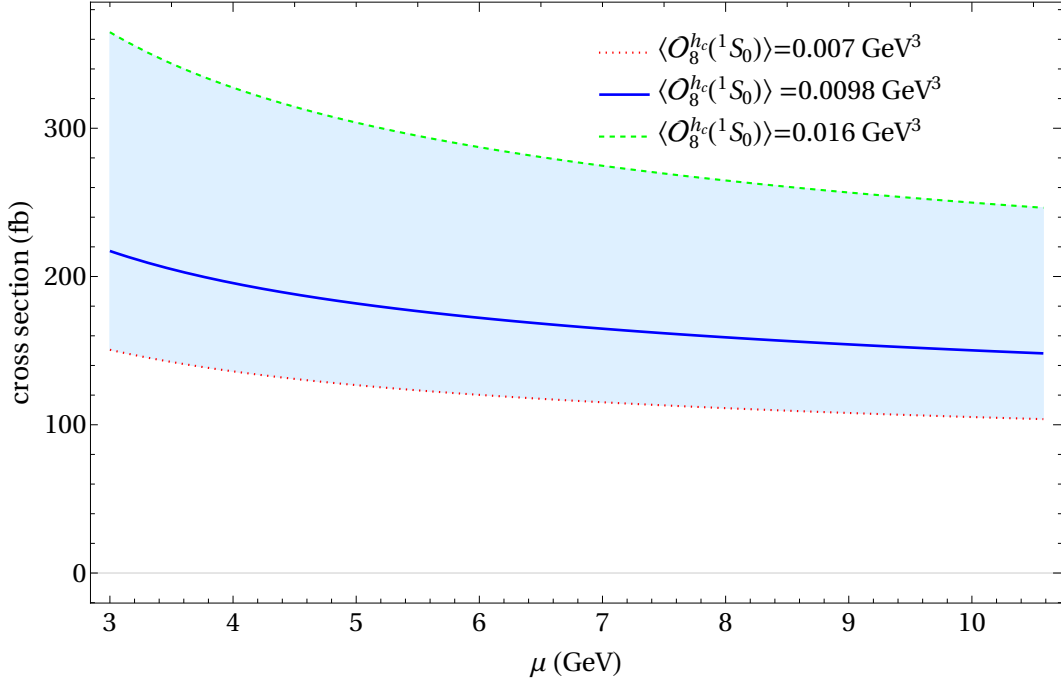


Figure 2: The dependence of total cross sections on the scale μ and color-octet LDME $\langle \mathcal{O}_8^{h_c(1P)}(^1S_0) \rangle$. The band represents the theoretical uncertainty due to the variation of the color-octet LDME.

V. NUMERICAL RESULTS

In this Section, we present the numerical predictions for the differential and total cross sections for the inclusive h_c production at Belle 2 experiment, $\sqrt{s} = 10.58$ GeV. We take the running QED coupling constant $\alpha(\sqrt{s}) = 1/130.9$ [58], the charm quark mass $m_c = 1.5$ GeV, the QCD renormalization scale $\mu = \sqrt{s}/2 = 5.29$ GeV and $\Lambda_{\text{QCD}} = 332$ MeV. For the color-singlet LDMEs of $h_c(1P)$, we take $\langle \mathcal{O}_1^{h_c(1P)}(^1P_1) \rangle = 0.32 \text{ GeV}^5$ [56]. For the color-octet LDMEs $\langle \mathcal{O}_8^{h_c(1P)}(^1S_0) \rangle$, we fix the NRQCD factorization scale to be $\mu_\Lambda = m_c$. However, this LDME bears a large uncertainty. In Table I, we present some benchmark choices of the octet LDMEs $\langle \mathcal{O}_8^{h_c(1P)}(^1S_0) \rangle$ and the corresponding integrated cross sections. In Fig. 2, we also show the dependence of the total cross section on the renormalization scale μ and the color-octet LDME. From Table I and Fig. 2, we find that the cross section of the inclusive h_c production rate at B factory energy is rather sensitive to the color-octet LDME. Therefore,

the future measurements of this inclusive h_c production at Belle 2 may provide a good place to unearth the value of this color-octet LDME. In the other places of the paper, we will fix the value of this color octet LDMEs as $\langle \mathcal{O}_8^{h_c(1P)}(^1S_0) \rangle = 0.0098 \text{ GeV}^3$.

In Fig. 3, we also show the scale dependence of the integrated cross section from each individual channel, at various perturbative level. The scale μ is varied from $2m_c$ to \sqrt{s} . From Table I and Fig. 3, one sees that the NLO QCD corrections to the color-octet channel are important, with a K -factor of about 1.8 and the color-octet contribution dominates the total production rate. It is noteworthy the color-singlet contribution in the $\overline{\text{MS}}$ scheme even becomes negative.

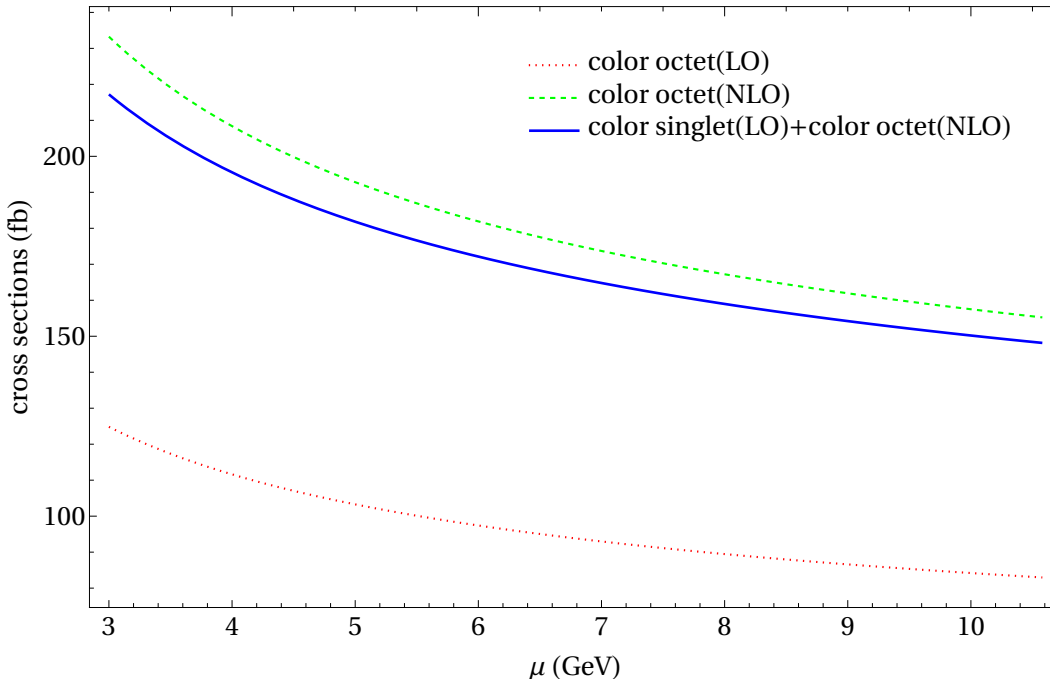


Figure 3: Variation of the total cross section for the inclusive h_c production with the renormalization scale μ , which ranges from $2m_c$ to \sqrt{s} .

To date, Belle 1 experiment has accumulated an integrated luminosity about 711 fb^{-1} at $\sqrt{s} = 10.58 \text{ GeV}$. Thus, from our calculation, around $(0.9 - 1.0) \times 10^5 h_c(1P)$ events should have already been produced. Furthermore, we expect that roughly $(6 - 7) \times 10^6 h_c(1P)$ events will be produced, when the designed luminosity reaches 50 ab^{-1} at $\sqrt{s} = 10.58 \text{ GeV}$ in the forthcoming Belle 2 experiment.

Such a huge dataset of h_c events may allow experimentalists to measure the h_c differential energy spectrum. The h_c energy distribution from fixed-order prediction is plotted in Fig. 4, where the end-point enhancement near $z \rightarrow 1 + r$ can be readily visualized. The end-point divergence clearly indicates the breakdown of the fixed-order perturbative prediction near the maximal energy of h_c .

For the color-octet channel, the large endpoint logarithms can be resummed to the NLL accuracy within the SCET framework, as was expounded in Section IV. Consequently, the endpoint divergence problem can be resolved accordingly. Away from the endpoint region, we merge the scales $\mu_S = \mu_H = \mu_J = \mu$ to turn off the resummation effect; on the other hand, while near the end point, we truncate the soft scale μ_S to around 1 GeV, to avoid the

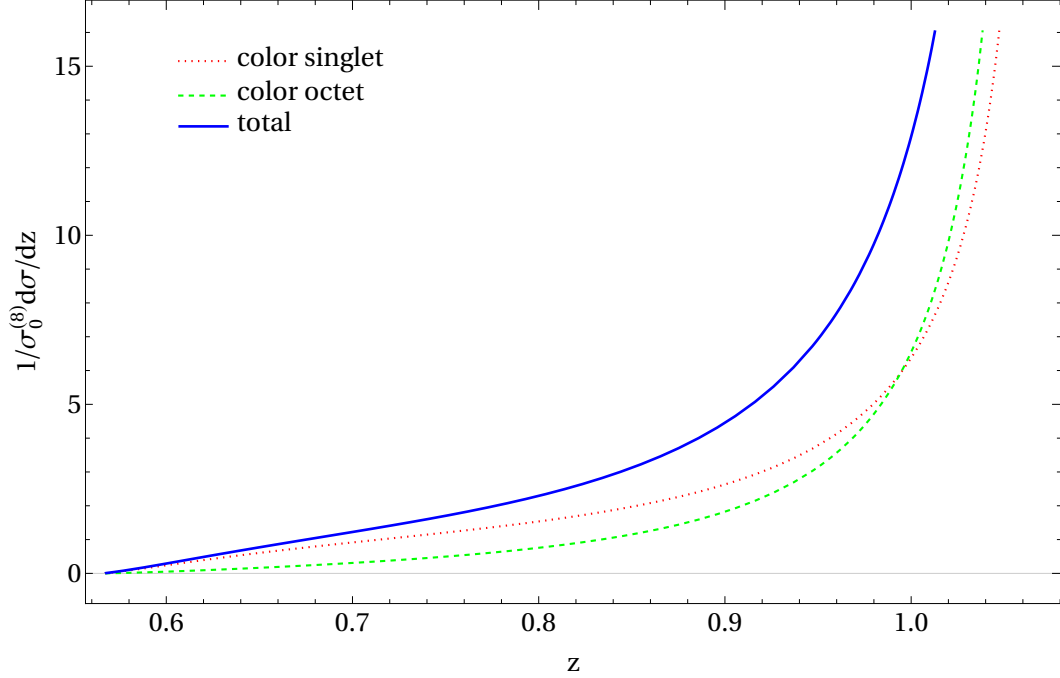


Figure 4: The h_c energy spectrum at $\sqrt{s} = 10.58$ GeV from the fixed-order calculation. In addition to their sum, we have also showed the contribution from the LO color-singlet channel and the NLO color-octet channel separately.

Landau pole. To account for the nonperturbative effects, we implement the non-perturbative shape function model following Ref. [32, 53]. We further match the NLL resummation with the NLO results to obtain the prediction for the full spectrum. The NLO + NLL cross section is plotted in Fig. 5, where the two sets of parameters for shape function are adopted, $(a = 5/2, b = 3/2)$ and $(a = 3, b = 2)$, respectively. We can see that the unphysical enhancement near the kinematic endpoint is removed after resummation.

It is curious whether and how the $h_c(2P)$ meson, the first radially-excited spin-singlet P -wave charmonium, could be observed at Super B factory. To reconstruct the potential $h_c(2P)$ events, one potential useful decay chain is $h_c(2P) \rightarrow \eta_c(2S)\gamma$, followed by $\eta_c(2S) \rightarrow h_c(1P)\gamma$, $h_c(1P) \rightarrow \eta_c\gamma$, and $\eta_c \rightarrow K^+K^-\pi^0$. These decay channels are relatively clean, which hopefully will be helpful for hunting the elusive $h_c(2P)$ state.

The above theoretical formulae can be readily transplanted to predict the inclusive production of $h_c(2P)$ meson. In order to predict the inclusive $h_c(2P)$ production rate, we adopt the color-singlet LDMEs $\langle \mathcal{O}_1^{h_c(2P)}(^1P_1) \rangle = 0.438 \text{ GeV}^5$ [19, 59]. It is rather difficult to accurately pin down the value of the color-octet LDME for $h_c(2P)$, and we follow the very rough estimation based on the renormalization-group equation in Ref. [19], and get the value $\langle \mathcal{O}_8^{h_c(2P)}(^1S_0) \rangle \approx 0.012 \text{ GeV}^3$. According to these inputs and ignoring the small difference in phase space integration, the total cross section of $h_c(2P)$ is estimated to be around $(0.15 - 0.16) \text{ pb}$ at $\sqrt{s} = 10.58 \text{ GeV}$. Around 10^5 and 7×10^6 $h_c(2P)$ events are expected, when the integrated luminosity reaches 711 fb^{-1} and 50 ab^{-1} at $\sqrt{s} = 10.58 \text{ GeV}$, respectively. The energy spectrum of the $h_c(2P)$ state assumes a similar shape as in plotted Fig. 5.

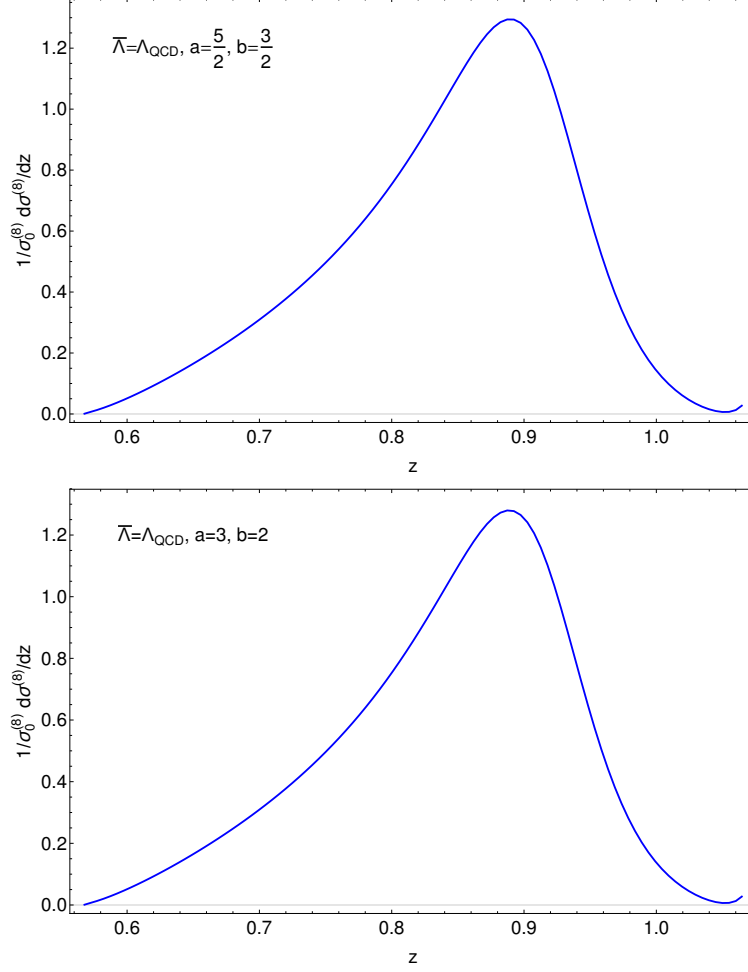


Figure 5: The solid curves are the NLO+NLL predictions for the h_c energy spectrum, convoluted with shape function as given in (42).

VI. SUMMARY

In this paper, we compute the NLO perturbative correction to the color-octet h_c inclusive production in e^+e^- annihilation at the B factory energy, within the NRQCD factorization framework. We are able to deduce the NLO color-octet SDC in a closed form. The NLO correction from the color-octet channel is found to be positive and important. Around 10^7 $h_c(1P)$ and $h_c(2P)$ events are expected with the projected 50 ab^{-1} luminosity at $\sqrt{s} = 10.58 \text{ GeV}$ in the forthcoming Belle 2 experiment. It will be interesting to observe these P -wave spin-singlet states in the inclusive production.

Nevertheless, the h_c energy spectrum predicted from our NLO calculation is plagued with the end-point enhancement, which implies the failure of fixed-order calculation near the maximal energy of h_c . With the aid of the SCET formalism, these large endpoint logarithms are resummed to the next-to-leading logarithmic accuracy. Consequently, in conjunction with the nonperturbative shape function models, we obtain the well-behaved predictions for the h_c energy spectrum in the entire kinematic range, which awaits the examination in the forthcoming Super Belle experiment.

Acknowledgments

We are grateful to Cheng-Ping Shen for several useful discussions on experimental aspects. X. L. would like to thank the Kavli Institute of Theoretical Physics in Santa Barbara for the hospitality during the completion of this manuscript. This work was supported in part by the National Natural Science Foundation of China under Grant No. 11375168, 11475188, 11621131001 (CRC110 by DGF and NSFC), and 11647163, by the Open Project Program of State Key Laboratory of Theoretical Physics under Grant No. Y4KF081CJ1, by the IHEP Innovation Grant under contract number Y4545170Y2, by the State Key Lab for Electronics and Particle Detectors, and by Natural Science Foundation of Jiangsu under Grant No. BK20171471, and by the Research Start-up Funding of Nanjing Normal University.

A. ANALYTIC INTEGRATION OVER THE THREE-BODY PHASE SPACE

The three-body phase space in $d = 4 - 2\epsilon$ dimensions can be expressed as [19]

$$\begin{aligned} \int d\Phi_3 &= \frac{c_\epsilon(4\pi)^\epsilon}{\Gamma(1-\epsilon)} \left(\frac{s}{2}\right)^{1-2\epsilon} \frac{1}{(4\pi)^3} \int_{2\sqrt{r}}^{1+r} dz \int_{a-b}^{a+b} dx_1 x_1^{-2\epsilon} (z^2 - 4r)^{-\epsilon} (1 - \cos^2 \theta)^{-\epsilon} \\ &= \frac{c_\epsilon(4\pi)^\epsilon}{\Gamma(1-\epsilon)} \left(\frac{s}{2}\right)^{1-2\epsilon} \frac{1}{(4\pi)^3} \int_{2\sqrt{r}}^{1+r} dz \int_{a-b}^{a+b} dx_1 2^{-2\epsilon} (1+r-z)^{-\epsilon} (x_1 - a + b)^{-\epsilon} (a + b - x_1)^{-\epsilon} \\ &= \frac{c_\epsilon(4\pi)^\epsilon}{\Gamma(1-\epsilon)} \frac{s^{1-2\epsilon}}{2} \frac{1}{(4\pi)^3} \int_{2\sqrt{r}}^{1+r} dz (1+r-z)^{-\epsilon} \int_{-b}^b d\eta (b+\eta)^{-\epsilon} (b-\eta)^{-\epsilon}, \end{aligned} \quad (\text{A.1})$$

where $a = \frac{2-z}{2}$, $b = \frac{\sqrt{z^2-4r}}{2}$ and θ is the angular between \mathbf{k}_1 and \mathbf{P} :

$$\cos \theta = \frac{2(1+r-z) - x_1(2-z)}{x_1 \sqrt{z^2-4r}}.$$

The second term $\mathcal{I}_{\text{SC}}(x_i, z)$ in Eq. (14) contains IR singularities when one of the final-state gluons become soft. Define:

$$\mathcal{A}_S = \int_{a-b}^{a+b} dx_1 \frac{(1+r-z)^{-\epsilon} (x_1 - a + b)^{-\epsilon} (a + b - x_1)^{-\epsilon}}{(1+r-z-x_1)^2}, \quad (\text{A.2})$$

and

$$t = \frac{1+r-z}{x_1}. \quad (\text{A.3})$$

Then

$$0 < a - b < t < a + b < 1 - r.$$

The integration in Eq. (A.2) can be expressed as

$$\begin{aligned} \mathcal{A}_S &= \frac{1}{(1+r-z)^{1+2\epsilon}} \int_{a-b}^{a+b} dt \frac{(t-a+b)^{-\epsilon} (a+b-t)^{-\epsilon} t^{2\epsilon}}{(1-t)^2} \\ &= \left\{ -\frac{1-r}{2r\epsilon} + \frac{(1-r)[4\ln(1-\sqrt{r}) + \ln r]}{2r} \right\} \delta(1+r-z) + \left[\frac{1}{1+r-z} \right]_+ \frac{\sqrt{z^2-4r}}{r}, \end{aligned} \quad (\text{A.4})$$

where we have expanded the $(1+r-z)^{-1-2\epsilon}$ as

$$\frac{1}{(1+r-z)^{1+2\epsilon}} = -\frac{\delta(1+r-z)}{2\epsilon(1-\sqrt{r})^{4\epsilon}} + \left[\frac{1}{1+r-z} \right]_+ - 2\epsilon \left[\frac{\ln(1+r-z)}{1+r-z} \right]_+ + \dots \quad (\text{A.5})$$

The divergence part of $\mathcal{I}_{\text{SC}}(x_i, z)$ in Eq. (14) can be separated into two parts:

$$\frac{1}{(1+r-z)(1+r-z-x_1)} = \frac{1}{x_1(1+r-z-x_1)} - \frac{1}{x_1(1+r-z)}. \quad (\text{A.6})$$

The first term in Eq. (A.6) corresponds to

$$\begin{aligned} \mathcal{A}'_{\text{S}} &= \int_{a-b}^{a+b} dx_1 \frac{(1+r-z)^{-\epsilon} (x_1-a+b)^{-\epsilon} (a+b-x_1)^{-\epsilon}}{x_1(1+r-z-x_1)} \\ &= \frac{1}{(1+r-z)^{1+2\epsilon}} \int_{a-b}^{a+b} dt \frac{(t-a+b)^{-\epsilon} (a+b-t)^{-\epsilon} t^{2\epsilon}}{t-1} \\ &= \left\{ -\frac{\ln r}{2\epsilon} + \frac{1}{4} [\ln^2 r + 8 \ln(1-\sqrt{r}) \ln r] \right\} \delta(1+r-z) + \left[\frac{1}{1+r-z} \right]_+ \ln \frac{z - \sqrt{z^2 - 4r}}{z + \sqrt{z^2 - 4r}}. \end{aligned} \quad (\text{A.7})$$

The second term in Eq. (A.6) contains soft and collinear singularities. Define:

$$\begin{aligned} \mathcal{A}_{\text{SC}} &= \int_{a-b}^{a+b} dx_1 \frac{(1+r-z)^{-\epsilon} (x_1-a+b)^{-\epsilon} (a+b-x_1)^{-\epsilon}}{x_1(1+r-z)} \\ &= \frac{1}{(1+r-z)^{1+\epsilon}} \int_{a-b}^{a+b} dx_1 \frac{(x_1-a+b)^{-\epsilon} (a+b-x_1)^{-\epsilon}}{x_1} \\ &= \frac{1}{(1+r-z)^{1+\epsilon}} \int_{-b}^b d\eta \frac{(\eta+b)^{-\epsilon} (b-\eta)^{-\epsilon}}{\eta+a}, \end{aligned} \quad (\text{A.8})$$

where

$$\begin{aligned} \int_{-b}^b d\eta \frac{(\eta+b)^{-\epsilon} (b-\eta)^{-\epsilon}}{\eta+a} &= \frac{\sqrt{\pi} b^{1-2\epsilon} \Gamma(1-\epsilon) {}_2F_1\left(\frac{1}{2}, 1; \frac{3}{2} - \epsilon; \frac{b^2}{a^2}\right)}{a \Gamma\left(\frac{3}{2} - \epsilon\right)} \\ &= \frac{\sqrt{\pi} b^{1-2\epsilon} \Gamma(-\epsilon) {}_2F_1\left(\frac{1}{2}, 1; 1 + \epsilon; 1 - \frac{b^2}{a^2}\right)}{a \Gamma\left(\frac{1}{2} - \epsilon\right)} + \pi \csc(\pi\epsilon) (a^2 - b^2)^{-\epsilon}. \end{aligned} \quad (\text{A.9})$$

We can expand the hypergeometric function in Eq. (A.9) with HypExp [60]:

$${}_2F_1\left(\frac{1}{2}, 1; 1 + \epsilon; 1 - \frac{b^2}{a^2}\right) = \frac{a}{b} \left(1 + 2\epsilon \ln \frac{2b}{a+b} \right) + \mathcal{O}(\epsilon^2). \quad (\text{A.10})$$

In Eq. (A.10), the $\mathcal{O}(\epsilon^2)$ term will finally vanish due to the δ function in Eq. (A.5), so it is legitimate to expand the hypergeometric function to $\mathcal{O}(\epsilon)$. With the trick shown in

Eq. (A.5), we can get

$$\begin{aligned}
& \frac{1}{(1+r-z)^{1+\epsilon}} \frac{\sqrt{\pi} b^{1-2\epsilon} \Gamma(-\epsilon) {}_2F_1\left(\frac{1}{2}, 1; 1+\epsilon; 1-\frac{b^2}{a^2}\right)}{a \Gamma\left(\frac{1}{2}-\epsilon\right)} \\
&= \left\{ \frac{1}{\epsilon^2} - \frac{2 \ln[(1-\sqrt{r})(1-r)]}{\epsilon} + 2 \ln^2[(1-\sqrt{r})(1-r)] - \frac{\pi^2}{6} \right\} \delta(1+r-z) \\
&+ \left[-\frac{1}{\epsilon} + 2 \ln\left(\frac{2-z+\sqrt{z^2-4r}}{2}\right) \right] \left[\frac{1}{1+r-z} \right]_+ + \left[\frac{\ln(1+r-z)}{1+r-z} \right]_+, \quad (\text{A.11a})
\end{aligned}$$

and

$$\begin{aligned}
& \frac{1}{(1+r-z)^{1+\epsilon}} \pi \csc(\pi\epsilon) (a^2-b^2)^{-\epsilon} \\
&= \left\{ -\frac{1}{2\epsilon^2} + \frac{2 \ln(1-\sqrt{r})}{\epsilon} - 4 \ln^2(1-\sqrt{r}) - \frac{\pi^2}{12} \right\} \delta(1+r-z) + \frac{1}{\epsilon} \left[\frac{1}{1+r-z} \right]_+ - 2 \left[\frac{\ln(1+r-z)}{1+r-z} \right]_+. \quad (\text{A.11b})
\end{aligned}$$

The total result for \mathcal{A}_{SC} :

$$\begin{aligned}
\mathcal{A}_{\text{SC}} &= \left\{ \frac{1}{2\epsilon^2} - \frac{2 \ln(1-r)}{\epsilon} - 4 \ln^2(1-\sqrt{r}) + 2 \ln^2[(1-\sqrt{r})(1-r)] - \frac{\pi^2}{4} \right\} \delta(1+r-z) \\
&+ 2 \ln\left(\frac{2-z+\sqrt{z^2-4r}}{2}\right) \left[\frac{1}{1+r-z} \right]_+ - \left[\frac{\ln(1+r-z)}{1+r-z} \right]_+. \quad (\text{A.12})
\end{aligned}$$

-
- [1] T. A. Armstrong *et al.*, Phys. Rev. Lett. **69**, 2337 (1992). doi:10.1103/PhysRevLett.69.2337
 - [2] M. Andreotti *et al.*, Phys. Rev. D **72**, 032001 (2005). doi:10.1103/PhysRevD.72.032001
 - [3] J. L. Rosner *et al.* [CLEO Collaboration], Phys. Rev. Lett. **95**, 102003 (2005) doi:10.1103/PhysRevLett.95.102003 [hep-ex/0505073].
 - [4] M. Ablikim *et al.* [BESIII Collaboration], Phys. Rev. Lett. **104**, 132002 (2010) doi:10.1103/PhysRevLett.104.132002 [arXiv:1002.0501 [hep-ex]].
 - [5] M. Ablikim *et al.* [BESIII Collaboration], Phys. Rev. D **86**, 092009 (2012) doi:10.1103/PhysRevD.86.092009 [arXiv:1209.4963 [hep-ex]].
 - [6] C. Patrignani *et al.* [Particle Data Group], Chin. Phys. C **40**, no. 10, 100001 (2016). doi:10.1088/1674-1137/40/10/100001
 - [7] I. Adachi *et al.* [Belle Collaboration], Phys. Rev. Lett. **108**, 032001 (2012) doi:10.1103/PhysRevLett.108.032001 [arXiv:1103.3419 [hep-ex]].
 - [8] W. E. Caswell and G. P. Lepage, Phys. Lett. **167B**, 437 (1986). doi:10.1016/0370-2693(86)91297-9
 - [9] G. T. Bodwin, E. Braaten and G. P. Lepage, Phys. Rev. D **51**, 1125 (1995) Erratum: [Phys. Rev. D **55**, 5853 (1997)] doi:10.1103/PhysRevD.55.5853, 10.1103/PhysRevD.51.1125 [hep-ph/9407339].
 - [10] N. Brambilla *et al.*, Eur. Phys. J. C **71**, 1534 (2011) doi:10.1140/epjc/s10052-010-1534-9 [arXiv:1010.5827 [hep-ph]].

- [11] V. A. Novikov, L. B. Okun, M. A. Shifman, A. I. Vainshtein, M. B. Voloshin and V. I. Zakharov, Phys. Rept. **41**, 1 (1978). doi:10.1016/0370-1573(78)90120-5
- [12] J. Z. Li, Y. Q. Ma and K. T. Chao, Phys. Rev. D **88**, no. 3, 034002 (2013) doi:10.1103/PhysRevD.88.034002 [arXiv:1209.4011 [hep-ph]].
- [13] G. T. Bodwin, E. Braaten, T. C. Yuan and G. P. Lepage, Phys. Rev. D **46**, R3703 (1992) doi:10.1103/PhysRevD.46.R3703 [hep-ph/9208254].
- [14] M. Beneke, F. Maltoni and I. Z. Rothstein, Phys. Rev. D **59**, 054003 (1999) doi:10.1103/PhysRevD.59.054003 [hep-ph/9808360].
- [15] S. Fleming and T. Mehen, Phys. Rev. D **58**, 037503 (1998) [AIP Conf. Proc. **452**, no. 1, 101 (1998)] doi:10.1063/1.57084, 10.1103/PhysRevD.58.037503 [hep-ph/9801328].
- [16] K. Sridhar, Phys. Lett. B **674**, 36 (2009) doi:10.1016/j.physletb.2009.02.051 [arXiv:0812.0474 [hep-ph]].
- [17] C. F. Qiao, D. L. Ren and P. Sun, Phys. Lett. B **680**, 159 (2009) doi:10.1016/j.physletb.2009.08.047 [arXiv:0904.0726 [hep-ph]].
- [18] J. X. Wang and H. F. Zhang, J. Phys. G **42**, no. 2, 025004 (2015) doi:10.1088/0954-3899/42/2/025004 [arXiv:1403.5944 [hep-ph]].
- [19] Y. Jia, W. L. Sang and J. Xu, Phys. Rev. D **86**, 074023 (2012) doi:10.1103/PhysRevD.86.074023 [arXiv:1206.5785 [hep-ph]].
- [20] J. X. Wang and H. F. Zhang, Phys. Rev. D **86**, 074012 (2012) doi:10.1103/PhysRevD.86.074012 [arXiv:1207.2416 [hep-ph]].
- [21] G. Chen, X. G. Wu, Z. Sun, X. C. Zheng and J. M. Shen, Phys. Rev. D **89**, no. 1, 014006 (2014) doi:10.1103/PhysRevD.89.014006 [arXiv:1311.2735 [hep-ph]].
- [22] L. B. Chen, J. Jiang and C. F. Qiao, Chin. Phys. C **39**, no. 10, 103101 (2015) doi:10.1088/1674-1137/39/10/103101 [arXiv:1505.00382 [hep-ph]].
- [23] R. Zhu, Phys. Rev. D **92**, no. 7, 074017 (2015) doi:10.1103/PhysRevD.92.074017 [arXiv:1507.02031 [hep-ph]].
- [24] F. Feng, S. Ishaq, Y. Jia and J. Y. Zhang, arXiv:1712.09986 [hep-ph].
- [25] A. Abulencia *et al.* [CDF Collaboration], Phys. Rev. Lett. **99**, 132001 (2007) doi:10.1103/PhysRevLett.99.132001 [arXiv:0704.0638 [hep-ex]].
- [26] R. Aaij *et al.* [LHCb Collaboration], Eur. Phys. J. C **71**, 1645 (2011) doi:10.1140/epjc/s10052-011-1645-y [arXiv:1103.0423 [hep-ex]].
- [27] G. Aad *et al.* [ATLAS Collaboration], Nucl. Phys. B **850**, 387 (2011) doi:10.1016/j.nuclphysb.2011.05.015 [arXiv:1104.3038 [hep-ex]].
- [28] V. Khachatryan *et al.* [CMS Collaboration], Eur. Phys. J. C **71**, 1575 (2011) doi:10.1140/epjc/s10052-011-1575-8 [arXiv:1011.4193 [hep-ex]].
- [29] B. Abelev *et al.* [ALICE Collaboration], Phys. Rev. Lett. **108**, 082001 (2012) doi:10.1103/PhysRevLett.108.082001 [arXiv:1111.1630 [hep-ex]].
- [30] T. K. Pedlar *et al.* [CLEO Collaboration], Phys. Rev. Lett. **107**, 041803 (2011) doi:10.1103/PhysRevLett.107.041803 [arXiv:1104.2025 [hep-ex]].
- [31] M. Ablikim *et al.* [BESIII Collaboration], Phys. Rev. Lett. **118**, no. 9, 092002 (2017) doi:10.1103/PhysRevLett.118.092002 [arXiv:1610.07044 [hep-ex]].
- [32] S. Fleming, A. K. Leibovich and T. Mehen, Phys. Rev. D **68**, 094011 (2003) doi:10.1103/PhysRevD.68.094011 [hep-ph/0306139].
- [33] C. W. Bauer, S. Fleming and M. E. Luke, Phys. Rev. D **63**, 014006 (2000) doi:10.1103/PhysRevD.63.014006 [hep-ph/0005275].
- [34] C. W. Bauer, S. Fleming, D. Pirjol and I. W. Stewart, Phys. Rev. D **63**, 114020 (2001)

- doi:10.1103/PhysRevD.63.114020 [hep-ph/0011336].
- [35] C. W. Bauer and I. W. Stewart, Phys. Lett. B **516**, 134 (2001) doi:10.1016/S0370-2693(01)00902-9 [hep-ph/0107001].
 - [36] C. W. Bauer, D. Pirjol and I. W. Stewart, Phys. Rev. D **65**, 054022 (2002) doi:10.1103/PhysRevD.65.054022 [hep-ph/0109045].
 - [37] C. W. Bauer, S. Fleming, D. Pirjol, I. Z. Rothstein and I. W. Stewart, Phys. Rev. D **66**, 014017 (2002) doi:10.1103/PhysRevD.66.014017 [hep-ph/0202088].
 - [38] M. Beneke, A. P. Chapovsky, M. Diehl and T. Feldmann, Nucl. Phys. B **643**, 431 (2002) doi:10.1016/S0550-3213(02)00687-9 [hep-ph/0206152].
 - [39] G. C. Nayak, J. W. Qiu and G. F. Sterman, Phys. Lett. B **613**, 45 (2005) doi:10.1016/j.physletb.2005.03.031 [hep-ph/0501235].
 - [40] G. C. Nayak, J. W. Qiu and G. F. Sterman, Phys. Rev. D **72**, 114012 (2005) doi:10.1103/PhysRevD.72.114012 [hep-ph/0509021].
 - [41] A. Petrelli, M. Cacciari, M. Greco, F. Maltoni and M. L. Mangano, Nucl. Phys. B **514**, 245 (1998) doi:10.1016/S0550-3213(97)00801-8 [hep-ph/9707223].
 - [42] W. Y. Keung, Phys. Rev. D **23**, 2072 (1981). doi:10.1103/PhysRevD.23.2072
 - [43] T. Hahn, Comput. Phys. Commun. **140**, 418 (2001) doi:10.1016/S0010-4655(01)00290-9 [hep-ph/0012260].
 - [44] V. Shtabovenko, R. Mertig and F. Orellana, Comput. Phys. Commun. **207**, 432 (2016) doi:10.1016/j.cpc.2016.06.008 [arXiv:1601.01167 [hep-ph]].
 - [45] Y. J. Zhang, Y. Q. Ma, K. Wang and K. T. Chao, Phys. Rev. D **81**, 034015 (2010) doi:10.1103/PhysRevD.81.034015 [arXiv:0911.2166 [hep-ph]].
 - [46] B. W. Harris and J. F. Owens, Phys. Rev. D **65**, 094032 (2002) doi:10.1103/PhysRevD.65.094032 [hep-ph/0102128].
 - [47] F. Feng, Comput. Phys. Commun. **183**, 2158 (2012) doi:10.1016/j.cpc.2012.03.025 [arXiv:1204.2314 [hep-ph]].
 - [48] A. V. Smirnov, Comput. Phys. Commun. **189**, 182 (2015) doi:10.1016/j.cpc.2014.11.024 [arXiv:1408.2372 [hep-ph]].
 - [49] T. Hahn and M. Perez-Victoria, Comput. Phys. Commun. **118**, 153 (1999) doi:10.1016/S0010-4655(98)00173-8 [hep-ph/9807565].
 - [50] S. Fleming, A. K. Leibovich, T. Mehen and I. Z. Rothstein, Phys. Rev. D **86**, 094012 (2012) doi:10.1103/PhysRevD.86.094012 [arXiv:1207.2578 [hep-ph]].
 - [51] Z. B. Kang, Y. Q. Ma, J. W. Qiu and G. Sterman, Phys. Rev. D **90**, no. 3, 034006 (2014) doi:10.1103/PhysRevD.90.034006 [arXiv:1401.0923 [hep-ph]].
 - [52] Y. Q. Ma, J. W. Qiu, G. Sterman and H. Zhang, Phys. Rev. Lett. **113**, no. 14, 142002 (2014) doi:10.1103/PhysRevLett.113.142002 [arXiv:1407.0383 [hep-ph]].
 - [53] A. K. Leibovich, Z. Ligeti and M. B. Wise, Phys. Lett. B **539**, 242 (2002) doi:10.1016/S0370-2693(02)02097-X [hep-ph/0205148].
 - [54] Y. Q. Ma, K. Wang and K. T. Chao, Phys. Rev. D **83**, 111503 (2011) doi:10.1103/PhysRevD.83.111503 [arXiv:1002.3987 [hep-ph]].
 - [55] B. Gong, L. P. Wan, J. X. Wang and H. F. Zhang, Phys. Rev. Lett. **110**, no. 4, 042002 (2013) doi:10.1103/PhysRevLett.110.042002 [arXiv:1205.6682 [hep-ph]].
 - [56] P. L. Cho and A. K. Leibovich, Phys. Rev. D **53**, 150 (1996) doi:10.1103/PhysRevD.53.150 [hep-ph/9505329].
 - [57] P. L. Cho and A. K. Leibovich, Phys. Rev. D **53**, 6203 (1996) doi:10.1103/PhysRevD.53.6203 [hep-ph/9511315].

- [58] G. T. Bodwin, J. Lee and C. Yu, Phys. Rev. D **77**, 094018 (2008) doi:10.1103/PhysRevD.77.094018 [arXiv:0710.0995 [hep-ph]].
- [59] E. J. Eichten and C. Quigg, Phys. Rev. D **52**, 1726 (1995) doi:10.1103/PhysRevD.52.1726 [hep-ph/9503356].
- [60] T. Huber and D. Maitre, Comput. Phys. Commun. **178**, 755 (2008) doi:10.1016/j.cpc.2007.12.008 [arXiv:0708.2443 [hep-ph]].